# Preparation and Characterization of Cellulose Nanocrystal Extraction From *Pennisetum hydridum* Fertilized by Municipal Sewage Sludge via Sulfuric Acid Hydrolysis

Xiaoshan Yu[1], Yu Jiang[1], Qitang Wu[1,2], Zebin Wei[1,2], Xianke Lin[1] and Yangmei Chen[1,2]*

[1]College of Natural Resources and Environment, South China Agricultural University, Guangzhou, China, [2]Guangdong Provincial Key Laboratory of Agricultural & Rural Pollution Abatement and Environmental Safety, South China Agricultural University, Guangzhou, China

This research focuses on the preparation of cellulose nanocrystals (CNCs) from *Pennisetum hydridum* fertilized by municipal sewage sludge (MSS) through sulfuric acid hydrolysis in different acid concentrations (40–65%), temperature (room temperature ~55°C), and reaction time (50–120 min). The results showed that the obtained CNC possessed stable dispersion in water. The length of CNCs reached 272.5 nm under the condition of room temperature (RT), 65% acid concentration, and 120 min reaction time, and the diameter was within 10 nm. Furthermore, Fourier transform infrared (FTIR) showed that the CNC still kept the cellulose type I structure. The crystallinity of CNCs increased to the maximum by 18.34% compared with that of delignified *Pennisetum hydridum* fibers. Thermogravimetry (TG) illustrated the thermal stability of CNCs was lower than that of delignified *Pennisetum hydridum* fibers due to the introduction of sulfate groups in the cellulose. This study demonstrated that *Pennisetum hydridum* fertilized by MSS might be a suitable raw material for CNCs. This implies meaningful resource utilization of MSS and *Pennisetum hydridum*.

Keywords: *Pennisetum hydridum*, cellulose nanocrystals, particle size, crystallinity, municipal sewage sludge

## INTRODUCTION

Nanocellulose is defined as a fiber material with at least one dimension size of 1–100 nm, which can be dispersed in water to form a stable colloid. Nanocellulose is a new fiber material whose diameter in microfiber units is in the nanoscale (2–100 nm) (Ru et al., 2017), the source of which is relatively broad, coming from gramineous plants, wood, cotton, tunicate animals, and bacteria. Due to its excellent mechanical properties, high specific surface area, high Young's modulus, renewability, biodegradability, and other advantages (Mao et al., 2017), nanocellulose has been widely used in

---

**Abbreviations:** CNC, cellulose nanocrystal; MSS, municipal sewage sludge; RT, room temperature; FTIR, Fourier transform infrared; TG, thermogravimetry; CNF, cellulose nanofibril; BNC, bacterial nanocellulose; ECC, electrospun cellulose; SEM, scanning electron microscopy; GSED, gaseous secondary electron detector; TEM, transmission electron microscopy; XRD, X-ray diffraction; CrI, crystallinity

the fields of biomedical products, nanocomposites, textiles, and new energy (Phanthong, et al., 2018; Liu et al., 2021; Liu et al., 2020).

The structure of cellulose consists of amorphous and crystalline regions. Due to the disordered structure of amorphous cellulose, the principle of separation of nanocellulose extracted from natural cellulose under the effect of chemicals or mechanical forces is the degradation of the fiber molecule of the amorphous area before the reaction of the crystalline region. It reserves the crystalline region structure, obtaining a nanoscale fiber with a high degree of crystallinity (Habibi et al., 2010). According to different material sources, fiber morphology, and preparation methods, nanocelluloses can be divided into four categories: cellulose nanocrystals (CNCs), cellulose nanofibrils (CNFs), bacterial nanocelluloses (BNCs), and electrospun celluloses (ECCs) (Liu et al., 2021).

At present, the common preparation methods of nanocellulose include sulfuric acid, hydrochloric acid, nitric acid, and other strong acid hydrolysis, TEMPO oxidation, mechanical method, biological enzyme method, and steam explosion method. Among them, TEMPO reagent is expensive. The oxidant is difficult to recover, and a large amount of wastewater will be produced in the preparation process (Visanko et al., 2014). The mechanical and explosive methods require special equipment with high energy consumption and low purity (Gao, 2011). Although the biological method has low energy consumption and meets the requirements of green and sustainable development, it has low efficiency and strict requirements on reaction conditions, which limits its large-scale application (Chen et al., 2012). The acid hydrolysis method is simple and mature. As early as 1947, there were studies on the preparation of CNCs by hydrolyzing cellulose with sulfuric acid (Nickerson and Habrle, 1947). Its degraded sugar by-products could also be fermented into biofuel. The method is simple, and at the same time, the acid could be recovered. Therefore, acid hydrolysis is still the main method for the rapid preparation of nanocellulose (Tang et al., 2014).

The genus of *Pennisetum hydridum* (hybrid giant Napier) is *Pennisetum*. It is bred by crossbreeding between *Pennisetum americanum* and elephant grass (Lin et al., 2015). It has a strong tillering ability, strong adaptability, fast growth, high yield, and high fiber content. As a new type of energy crop with high efficiency and economy, it has attracted attention. It is often used in animal husbandry feed (Peng et al., 2010) and pulp or paper manufacturing (Jiang et al., 2019). In recent years, it has also been used in soil and water conservation, ecological environment degradation control, and other environmental control aspects (Zhao et al., 2015). There have been studies on the use of biochar prepared from *Pennisetum hydridum* to treat urban sewage (Zhao et al., 2017) and heavy metal sewage (Huang et al., 2016). The purpose of remediation of heavy metal–contaminated soil was obtained by planting *Pennisetum hydridum* to enrich heavy metals in the soil (Yi et al., 2014; Wang et al., 2015; Xie et al., 2016; He et al., 2017), and the red mud and saline soil were improved (Ma et al., 2012; Ma et al., 2013).

A lot of research has been done on the extraction of nanocellulose from natural plant resources, including sisal, kapok, pineapple leaves, coconut husks, rice husks, bamboo, hemp, and industrial denim waste (Dai 2011; Nurain et al., 2012; Wang 2013; Deepa et al., 2015; Culsum 2021). *Pennisetum hydridum* as large biomass of plant [90–105 t (air-dried)/hm$^2$] may be an ideal raw material for the preparation of nanocellulose (He et al., 2020). However, a lot of *Pennisetum hydridum* is discarded or burned directly, causing resource waste and environmental pollution (Huang et al., 2016). It is a new way of resource recycling used by the preparation of nanocellulose from *Pennisetum hydridum*.

Therefore, CNCs were firstly prepared from *Pennisetum hydridum* of the non-wood fiber raw material fertilized by MSS in this study. Many studies used two steps for the pretreatment of raw materials to obtain CNCs (Bano and Negi, 2017). One step is firstly used for the removal of lignin and the other step for the removal of hemicellulose. We used a one-step method to obtain CNCs in this study, i.e., the removal of lignin using sodium chlorite. Furthermore, the particle size, chemical structure, crystal structure, fiber morphology, and thermal degradation performance of CNCs were evaluated. This study could provide meaningful reference data for the research and application of CNCs obtained from *Pennisetum hydridum*.

## MATERIALS AND METHODS

### Materials
The method of cultivation of *Pennisetum hydridum* using municipal sludge sewage was the same as that in our previous work (Jiang et al., 2019). Stalks of *Pennisetum hydridum* were harvested after 6 months. The *Pennisetum hydridum* stalks were ground and sifted after equilibrium moisture was achieved. The powder of *Pennisetum hydridum* that passed a 40-mesh sieve but was retained on a 60-mesh sieve was collected and put into a storage jar to be kept at room temperature.

### Pretreatment of Raw Material
Lignin of the powder of *Pennisetum hydridum* was removed by the traditional sodium chlorite method. The steps were as follows. An amount of 10 g *Pennisetum hydridum* powder was loaded into a 500 ml beaker, and 325 ml distilled water was added at a ratio of 1:32.5. The mixture was placed in a thermostat water bath at 75°C for 4 h, an amount of 3 g sodium chlorite was added every 1 h, and then glacial acetic acid was added to adjust the pH to 4.5. The above steps were repeated four times until the sample became white. The sample was placed in an extractor and cleaned with distilled water, repeatedly, until the filtrate pH was 7. The obtained delignified *Pennisetum hydridum* fiber was dried in an oven at 50°C.

Lignin and pentosane (hemicellulose) of the original *Pennisetum hydridum* and delignified sample were determined according to GB/T 2677.8-1994 and GB/T 2677.9-1994, respectively. The cellulose content was determined by the nitrate method.

## Preparation of Cellulose Nanocrystals

An amount of 3 g delignified *Pennisetum hydridum* fiber was mixed with sulfuric acid (30 ml) with a certain mass fraction (40, 55, and 65% wt), and the reaction was carried out in a Thermostat Ultrasonic Cleaner (SB-5200 DTD, Xinzhi Biological Technology Co., Ltd., Ningbo, China) at 40°C, 55°C, 70°C, and room temperature (RT, 25°C) for a certain period (50 min, 120 min). The frequency and power of the ultrasound were 40 Hz and 50 kW. The reaction product was centrifuged using a centrifuge (LL5-2A, Beijing Medical Centrifuge Factory, China) for 15 min at 5,310 × g, and the supernatant was removed. The supernatant was repeatedly centrifuged several times until the pH of the solution was about 6, and the supernatant became turbid. A certain amount of dried solid samples were taken to obtain CNCs.

## Particle Size and Zeta Potential Analysis

2 ml CNC sample solution was taken, diluted 100 times using deionized water, dispersed with ultrasonic treatment, and dropped into the sample pool. The particle size and zeta potential were measured using the Malvern laser particle analyzer (Nano ZS90, Malvern Instruments Co., Ltd., United Kingdom). The reported results were the average of two measurements.

## The Yield of CNCs

The obtained CNC suspension was dried to a constant weight at 50°C for at least 8 h in an oven and weighed after drying. The yield of CNCs was calculated as follows:

$$Y = \frac{m_2}{m_1} \times 100\%, \tag{1}$$

where Y is the yield of CNCs, %; $m_2$ is the weight of CNCs after drying, g; and $m_1$ is the weight of the original *Pennisetum hydridum*, g.

## Scanning Electron Microscopy Analysis of *Pennisetum hydridum* Fiber

The *Pennisetum hydridum* fiber was fixed on the observation table with copper adhesive conductive tape. A small amount of powder was sprinkled on the conductive adhesive and plated with gold. SEM imaging (XL-30-ESEM, FEI Corporation, Holland) was conducted using a gaseous secondary electron detector (GSED) at a temperature of about 23°C, accelerating voltage of 10–20 kV, and pressure of 800 Pa in the sample chamber. SEM images at different scales of 200, 100, and 10 μm were obtained, and their contrast and brightness were adjusted.

## Transmission Electron Microscopy Analysis

The CNC solution was dispersed evenly by ultrasonic treatment (power 600 W, shaking time 2 s, interval time 1 s, and duration of shaking 10 min), 10 μL solution was absorbed and dipped onto a carbon film copper mesh (200 mesh), and the excess liquid was absorbed by a clean filter paper. After a few minutes, a 10 μL 3% phosphotungstate stain (pH 7) was adsorbed and dropped onto

**TABLE 1 |** Components of *Pennisetum hydridum* before and after delignification.

| Components | Cellulose (%) | Lignin (%) | Hemicellulose |
|---|---|---|---|
| Before delignification | 40.8 | 20.4 | 23.5 |
| After delignification | 50.9 | 6.5 | 24.1 |

the copper net for negative staining for 5 min, the missing liquid was absorbed by a clean filter paper, and then the sample was dried naturally. The sample was observed using TEM under 80 kV acceleration voltage (Tecnai 12, FEI Corporation, Holland). 50 nanofibers were measured for the morphological analysis.

## Fourier Transform Infrared Spectrometry Analysis

The amounts of 1 mg CNC powder and 100 mg KBr were mixed and ground, and the mixture was pressed into a high-transparency tablet with a diameter of 13 mm by the tablet pressing method and then tested by FTIR (Vertex 70, Bruker Corporation, Germany) in the range of 4,000–500 $cm^{-1}$, with an accumulation of 64 scans and a resolution of 4 $cm^{-1}$.

## X-Ray Diffraction Analysis

The crystal structure of CNCs was analyzed by XRD (Ultima IV, Rigaku Corporation, Japan). The analyzing conditions were Cu-Kα source, 40 kV, and $\lambda = 0.154$. The scanning range was 5°–40°, with a scanning step width of 0.020° per scan. The crystallinity (CrI) was calculated by the Segal empirical formula (Chen et al., 2018) as

$$CrI, \% = \frac{I_{002} - I_{am}}{I_{002}} \times 100, \tag{2}$$

where $I_{002}$ is the maximum diffraction intensity of the cellulose (002) crystal plane and $I_{am}$ is the diffraction intensity of the non-crystalline zone between the 002 peak and the 101 peak.

## Thermogravimetric Analysis

An amount of 10 mg sample was taken and tested by a thermogravimetric analyzer (STA449 F3, NETZSCH Corporation, Germany). The analysis conditions were nitrogen atmosphere, a room temperature of 600°C, and a heating rate of 10°C/min.

# RESULTS AND DISCUSSION

## Chemical Components of Materials

The basic chemical components of *Pennisetum hydridum* before and after delignification are shown in **Table 1**. The cellulose content of *Pennisetum hydridum* after delignification reached 50.9%, which showed *Pennisetum hydridum* could be a good material for the production of nanocellulose. The lignin content of *Pennisetum hydridum* after delignification became very low. The hemicellulose content of *Pennisetum hydridum* after delignification became 24.1%.

**FIGURE 1 |** Flowchart of CNC production.
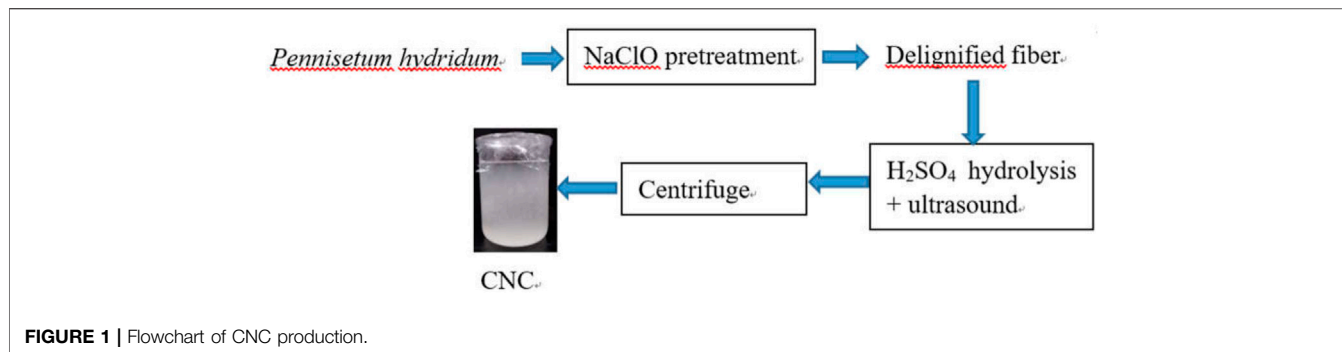
**TABLE 2 |** Particle size, zeta potential, and yield of CNCs at 40°C.

| $H_2SO_4$ (%) | Time (min) | Particle size (nm) | Zeta potential (mV) | Yield (%) |
|---|---|---|---|---|
| 40 | 50 | 447.6 | −22.9 | 31.0 |
| | 120 | 439.7 | −17.8 | 34.3 |
| 55 | 50 | 438.4 | −22.5 | 40.3 |
| | 120 | 422.2 | −27.4 | 43.6 |
| 65 | 50 | 624.9 | −28.4 | 35.6 |
| | 120 | 620.2 | −32.6 | 34.8 |

**TABLE 3 |** Particle size, zeta potential, and yield of CNCs at 55°C.

| $H_2SO_4$ (%) | Time (min) | Particle size (nm) | Zeta potential (mV) | Yield (%) |
|---|---|---|---|---|
| 40 | 50 | 625.1 | −15.3 | 41.4 |
| | 120 | 551.9 | −20.8 | 42.2 |
| 55 | 50 | 722.1 | −35.5 | 37.5 |
| | 120 | 467.6 | −33.0 | 37.0 |
| 65 | 50 | 668.1 | −29.7 | 26.4 |
| | 120 | 409.3 | −27.0 | 23.2 |

**TABLE 4 |** Particle size, zeta potential, and yield of CNCs at RT.

| $H_2SO_4$ (%) | Time (min) | Particle size (nm) | Zeta potential (mV) | Yield (%) |
|---|---|---|---|---|
| 40 | 50 | 355.0 | −23.1 | 32.5 |
| | 120 | 406.6 | −28.8 | 35.6 |
| 55 | 50 | 459.2 | −35.9 | 35.6 |
| | 120 | 278.0 | −36.9 | 36.8 |
| 65 | 50 | 369.8 | −34.2 | 35.3 |
| | 120 | 272.5 | −34.9 | 38.2 |

## Particle Size, Zeta Potential, and Yield of CNCs

The flowchart of the CNC production process used in this work is presented in **Figure 1**. The preparation method of nanocellulose is mainly to decompose large cellulose molecules into smaller nanocellulose molecules through physical crushing and chemical deconstruction (Du et al., 2018), which is known as the top-down approach (Nechyporchuk et al., 2016). Sulfuric acid hydrolysis is the earliest inorganic acid hydrolysis method of CNCs. Later, there have been studies to prepare CNCs by hydrolysis of hydrochloric acid, phosphoric acid, and other inorganic acids

(Kontturi et al., 2016; Espinosa et al., 2013; Vanderfleet et al., 2018).

Three treatment variables (treatment temperature, sulfuric acid mass fraction, and treatment time) were set in this study. After sulfuric acid hydrolysis for a certain period, the amorphous structure of cellulose was decomposed to obtain cellulose with a smaller size (Liu et al., 2017). As shown in **Tables 2, 3, 4**, the acid-hydrolyzed products under all conditions reached the nanometer size, and the mean particle size of CNCs was the smallest under RT, 65% wt $H_2SO_4$, and 120 min (**Figure 2A**; **Table 4**). When the other treatment conditions were the same, the longer the acid
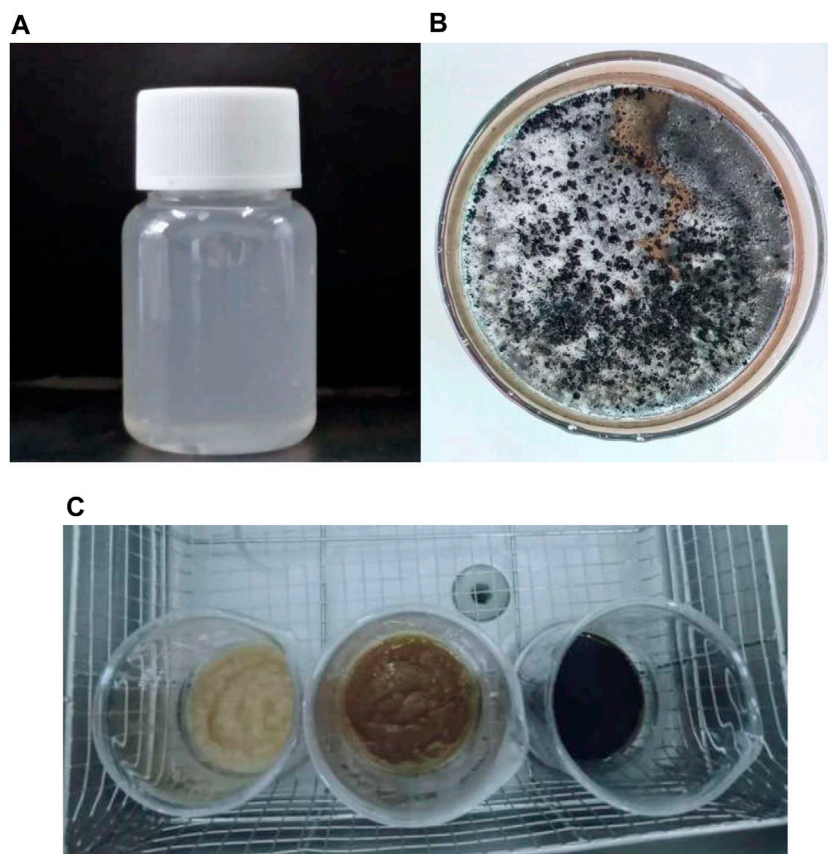
**FIGURE 2 |** CNC pictures at different treatment conditions: **(A)** CNC solution (RT); **(B)** carbonization (70°C); **(C)** color change of the CNC at 55°C under different $H_2SO_4$ mass fractions (from left to right: 40% wt, 55% wt, and 65% wt).

hydrolysis time, the smaller the particle size of the CNC. In general, the CNC prepared at room temperature had the smallest particle size compared to that at other temperatures when the other treatment conditions were the same. The particle size of the CNC was highest under 40°C and 65% $H_2SO_4$, as shown in **Table 2**. This may be caused by overreaction resulting in the partial flocculation of glucose generated by decomposition and carbonization of cellulose.

Different colors of production are shown due to the difference in the mass fraction of sulfuric acid (**Figure 2C**). When the temperature reaches 70°C and the mass fraction of sulfuric acid ≥ 55%, the product carbonizes and the color turns black (**Figure 2B**), so the measurement results of the product obtained at 70°C are not listed.

The zeta potential is used to measure the strength of repulsion or attraction between particles, which is an important parameter of the characterization of colloid system stability (Qin, 2018). Usually, the greater the zeta potential, the greater the stability of the colloid system. In most of the colloid systems, 30 mV is called the stability threshold. The zeta potential is higher than the threshold; strong electrostatic repulsion can prevent particles from getting close, thus increasing their stability (Qin, 2018). If the zeta potential is between −15 and 15 mV, the gel will condense. Due to the addition of sulfuric acid, the resulting

nanocrystals have sulfuric acid ester groups on the surface, which is negatively charged (Xu et al., 2016). It can be seen from **Table 2** that the zeta potential of CNCs obtained under all conditions is negative, and the absolute value is above 15 mV, which indicates that the prepared CNCs have good stability.

As shown in **Table 4**, the CNC yield was higher when the mass fraction of sulfuric acid was 65%, and the CNC yield increased with the increase of treatment time under the same mass fraction of sulfuric acid. When the temperature rises to 40°C, the yield of CNCs increases first and then decreases with the increase of sulfuric acid mass fraction. When the temperature is 55°C, the yield of CNCs increases first and then decreases with the increase of sulfuric acid. This is because of the different results produced by the interaction of temperature, sulfuric acid mass fraction, and time (Tang et al., 2011).

Although CNCs can be prepared from various cellulose sources and hydrolysis conditions, the conditions are not ideal, the yield and charge content may be very low, or the agglomeration may be caused by large CNC particles (Vanderfleet et al., 2018). It is generally concluded from previous studies that, by increasing time, temperature, and acid concentration, hydrolysis would be more intense, CNCs with a higher sulfate content and smaller size would be produced, and the yield would be higher (Beck-candanedo et al., 2005).
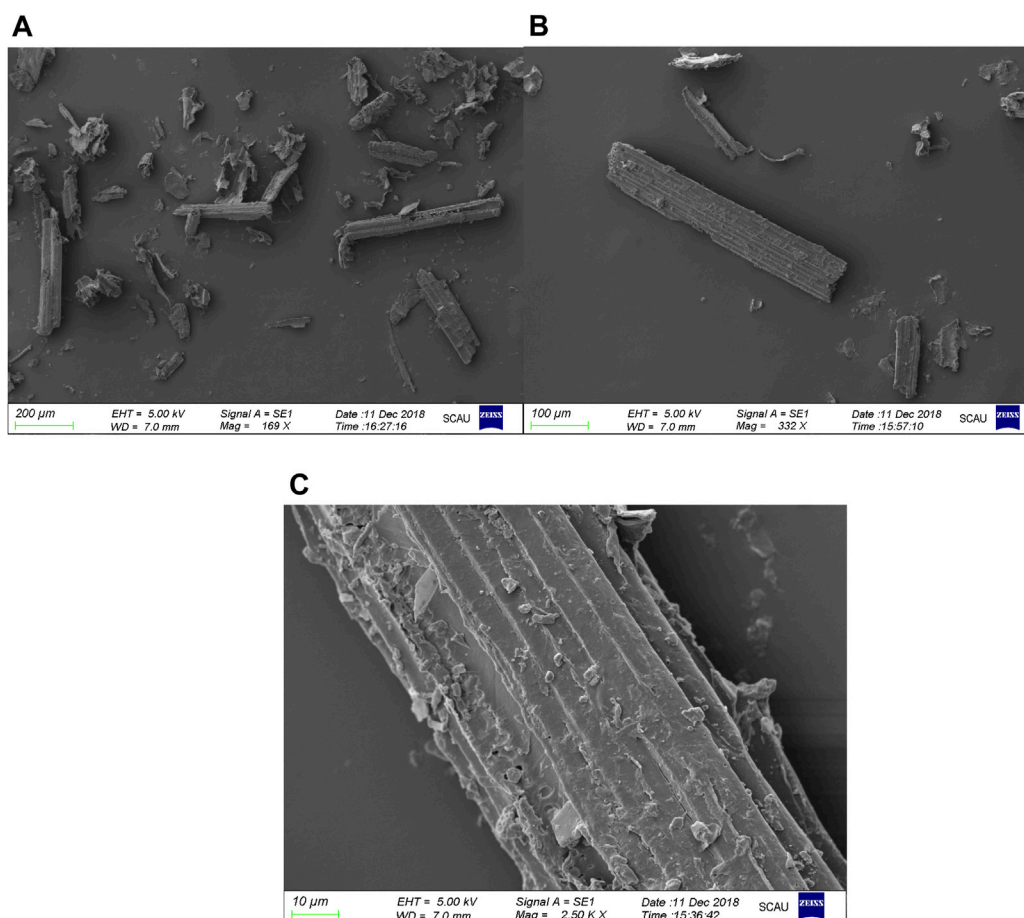
**FIGURE 3 |** SEM images of the *Pennisetum hydridum* fiber at different scales: **(A)** 200 µm; **(B)** 100 µm; **(C)** 10 µm.

However, if the intensity of hydrolysis exceeds a certain point, the crystallinity of CNC would be damaged, cellulose would be degraded into sugar, and furfural would be formed further (Wang, 2014), which would also lead to the decrease of CNC yield and the increase of by-products (Agarwal, 2015). In this study, CNCs were not obtained when hydrolyzed at 70°C with a higher concentration of sulfuric acid, which indicated that hydrolysis was too severe and the experimental conditions should be adjusted.
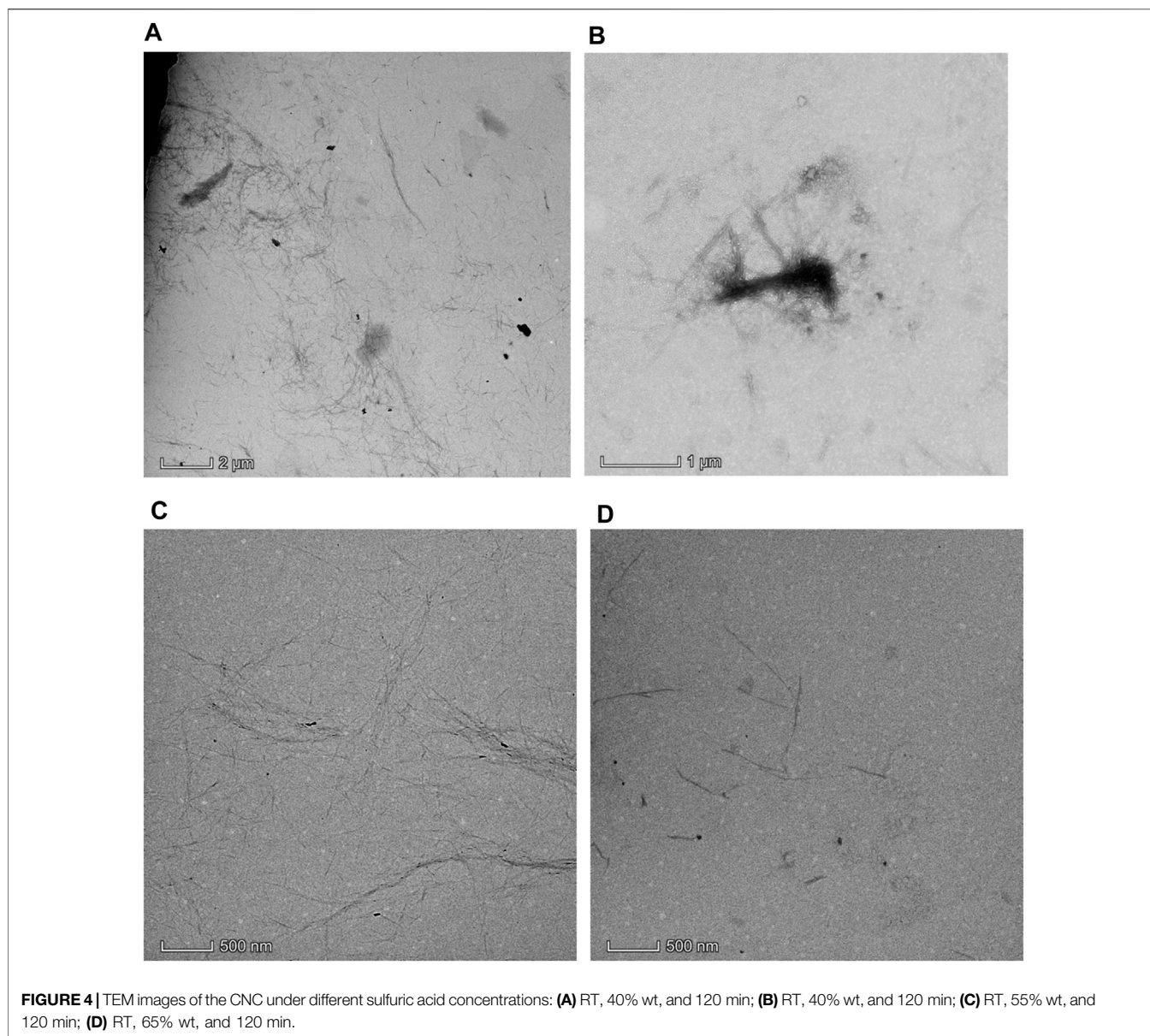
## Electron Microscopy Analysis of CNCs

From images of SEM, it can be seen that the length and width of the *Pennisetum hydridum* fiber were within 100 µm and about 10 µm, respectively (**Figure 3**). The average particle size of CNCs was around 400 nm under different acid hydrolysis conditions (**Tables 2**, **3**, **4**), and the difference was not big. Therefore, a few samples were observed by TEM (**Figures 2A,B**: RT, 40% wt, and 120 min; **Figure 2C**: RT, 55% wt, and 120 min; **Figure 2C**: RT, 65% wt, and 120 min). From **Figure 4**, it can be seen that the fiber length of CNCs was within 500 nm and the diameter was within 10 nm. Under the conditions of sulfuric acid concentration of 40 and 55% wt, there were some fiber bundles formed between celluloses, and it

was not easy to observe a single CNC. It can be seen that CNCs at the concentration of 65% wt sulfuric acid had the smallest length, were relatively uniform, and had the best dispersion. This might be due to the degradation of more amorphous cellulose of fiber as the acid concentration increases. Mukherjee (1953) was the first person to use TEM to obtain images of CNCs from sulfuric acid hydrolysis and observed rod-like particles of about 200 nm length and 10–20 nm diameter, which were consistent with the TEM images of CNCs prepared in this study (**Figure 4**).

## FTIR Analyses of Chemical Structures of CNCs

The chemical structure analysis of the delignified/bleached *Pennisetum hydridum* fiber and CNCs prepared at different temperatures was carried out by FTIR (**Figure 5**). The absorption bands and the corresponding structure assignments from the infrared spectra are based on literature values (Chen et al., 2013). From **Figure 5**, it can be seen that there was a major peak near $3,390\ cm^{-1}$ with the presence of -OH and C-H absorption peaks near $2,918\ cm^{-1}$ and a C-O absorption peak near $1,060\ cm^{-1}$. These main characteristic peaks did not change

**FIGURE 4 |** TEM images of the CNC under different sulfuric acid concentrations: **(A)** RT, 40% wt, and 120 min; **(B)** RT, 40% wt, and 120 min; **(C)** RT, 55% wt, and 120 min; **(D)** RT, 65% wt, and 120 min.

significantly, indicating that the CNC still had the basic structure of cellulose after acid hydrolysis.

The appearance of the asymmetrical S=O vibration associated with the C-O-SO$_3$ group in the CNC samples was approximately 1,250 cm$^{-1}$ and the appearance of the symmetrical C-O-SO$_3$ vibration was approximately 833 cm$^{-1}$ (Gu et al., 2013). There were some bands between 750 and 1,000 cm$^{-1}$ and other bands around 1,350 and 1,175 cm$^{-1}$, which indicated the presence of sulfonates in the CNC samples (Morais et al., 2013).

The main feature of the CNC samples was the appearance of the band at 1,730 cm$^{-1}$ related to carbonyl groups (C=O) from hemicellulose or esterification of cellulose (Liu et al., 2017). The band of CNCs prepared at 55°C at 1,163 cm$^{-1}$ assigned to C-O in lignin and xylan disappeared, which demonstrated that the lignin or hemicellulose was reduced during the acid hydrolysis procedure with the increasing reaction temperature.

The relative intensity of the band at 1,100 cm$^{-1}$ related to crystalline cellulose was increased in the CNC samples; however, the relative intensity of the band at 900 cm$^{-1}$ related to amorphous cellulose was decreased. It demonstrated that the ratio of crystalline to amorphous cellulose significantly increased after acid hydrolysis.

## Crystal Structure of CNC Analysis

Cellulose is composed of the crystalline zone and amorphous zone. The percentage of the crystalline zone as a whole of cellulose is crystallinity. Above cellulose's microproperties, it is very important to study the crystallinity of CNCs. As shown in **Figure 6**, the 002 crystal plane diffraction peak of cellulose I appeared near 22°. The diffraction angle overlapped each other between 101 and 10Ī crystal planes of cellulose I forming the broad diffraction peak during 14.5–17°. It is not hard to find that
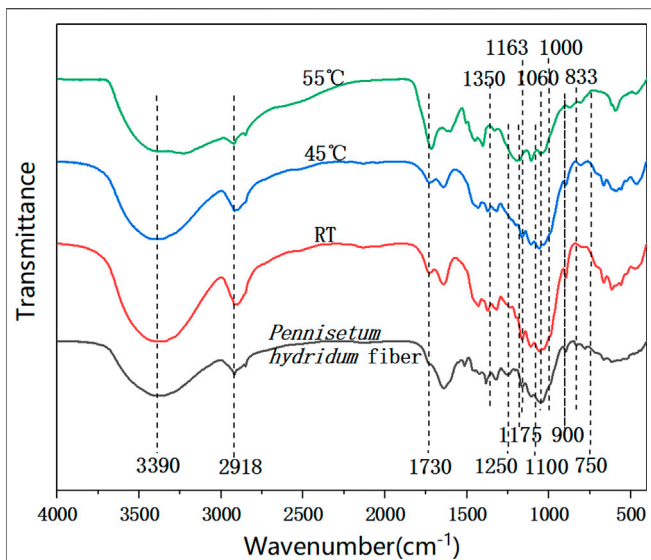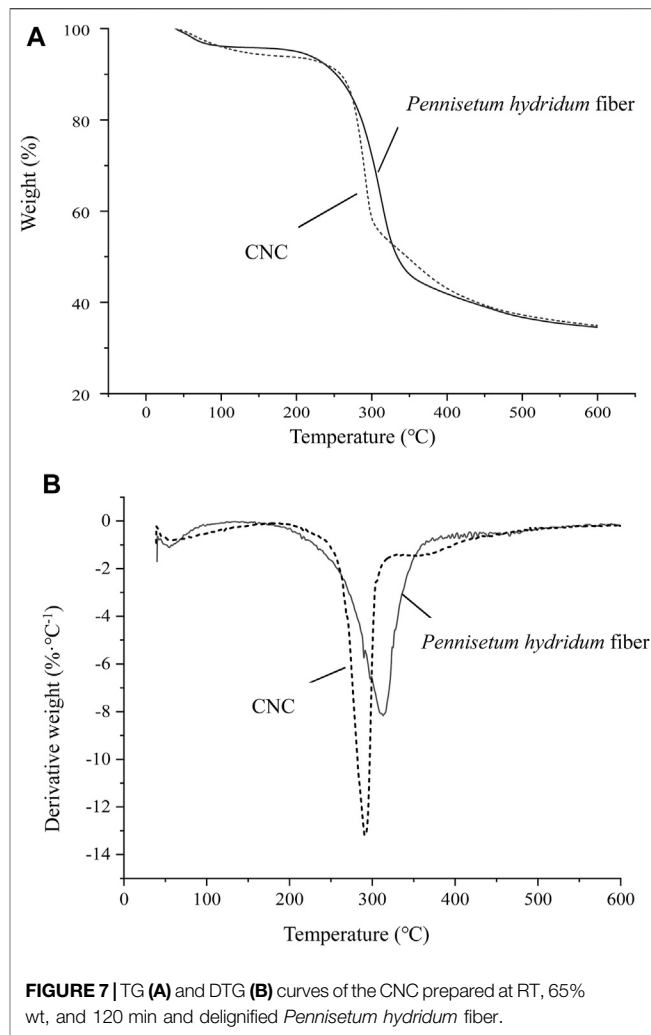
**FIGURE 5 |** FTIR spectra of the delignified *Pennisetum hydridum* fiber and CNC prepared at different temperatures: **(A)** *Pennisetum hydridum* fiber; **(B)** CNC prepared at RT, 65% wt, and 120 min; **(C)** CNC prepared at 40°C, 65% wt, and 120 min; **(D)** CNC prepared at 55°C, 65% wt, and 120 min.
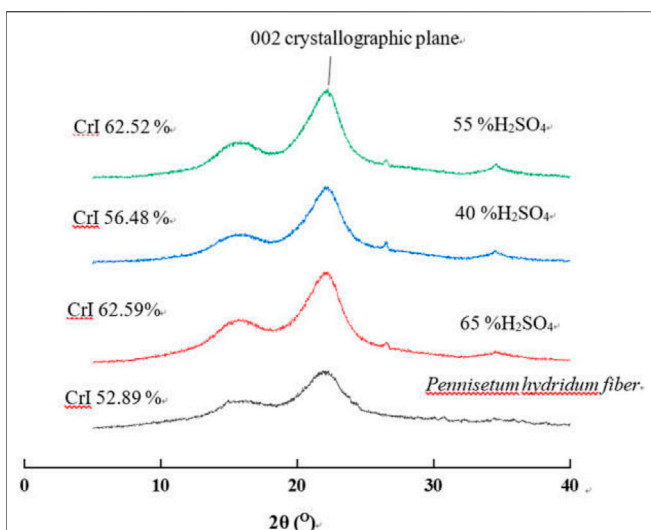


**FIGURE 6 |** XRD patterns of the CNC at different sulfuric acid concentrations (other conditions: RT, 120 min).



**FIGURE 7 |** TG **(A)** and DTG **(B)** curves of the CNC prepared at RT, 65% wt, and 120 min and delignified *Pennisetum hydridum* fiber.

the peak patterns of the CNC and delignified *Pennisetum hydridum* fiber were the same after sulfuric acid hydrolysis. They retained the crystal structure of cellulose I and have been changed. This is because the amorphous region of cellulose is damaged during sulfuric acid hydrolysis, which is consistent with the results of FTIR. The CrI of CNCs increased with the increase of the mass fraction of sulfuric acid due to the hydrolysis of amorphous cellulose. Compared with that of the *Pennisetum hydridum* fiber, the crystallinity of the CNC prepared with the mass fraction of sulfuric acid of 40, 55, and 65% wt increased by

6.79, 18.21, and 18.34%, respectively, and the maximum crystallinity reached 62.59% when $H_2SO_4$ was 65% wt.

## Thermogravimetric Analysis of CNCs

During the heating process, the structure of cellulose will be changed and the crystalline zone will be destroyed and even carbonized, finally. The relationship between the sample quality and the temperature change was tested by a thermal analyzer. As shown in **Figure 7**, when the temperature was below 200°C, that stage was mainly the process of water evaporation. TG curves of the CNC and *Pennisetum hydridum* fiber showed a small weight loss ratio, but the CNC (−6.06%) had more weight loss than the *Pennisetum hydridum* fiber (−4.02%) because of its better absorption. The stage of 250–400°C was the process of mass weight loss, and the structure of cellulose was decomposed into various volatile substances. The CNC first exhibited a degradation peak (291.1°C); this is because the presence of sulfur ester groups accelerated the pyrolysis process. When the temperature increased above 400°C, the degradation of cellulose was finished, and the residual masses of the CNC and *Pennisetum hydridum* fiber were equal. The CNC exhibited lower thermal stability compared to the *Pennisetum hydridum* fiber. This is

consistent with the research results of Xu (2016), in which the thermal stability of nanocellulose obtained from palm sheath is significantly lower than that of raw materials. The main reason for this might be linked to disruption of its crystalline structure and the introduction of sulfate groups during sulfuric acid hydrolysis. Moreover, smaller fiber dimensions, leading to higher surface areas exposed to heat, also have negative effects on thermal stability (Widsten et al., 2014).

Thermal stability is also an important parameter that is often considered in applications of materials. Kargarzadeh (2012) studied the influence of hydrolysis conditions on the thermal stability of CNCs obtained from kenaf bast fibers using sulfuric acid. A continuous and progressive decrease in the thermal stability of the nanoparticles occurred as the hydrolysis time increased, probably because of the high sulfation rate demonstrated by the zeta potential measurements (Kargarzadeh et al., 2012). Although reducing the hydrolysis time could improve thermal stability, the size of CNCs produced was larger and the colloid stability was lower. The experimental results of this study also indicated that the size of the CNC was smaller when the hydrolysis time was longer because of degradation of the amorphous region.

## CONCLUSION

In this study, the production of CNC-based *Pennisetum hydridum* fiber using ultrasound-assisted sulfuric acid hydrolysis was investigated. The highest yield of CNCs was 43.6%. The fiber length of CNCs was within 500 nm, and the diameter was within 10 nm. CNCs still had the basic structure of cellulose after acid hydrolysis. The significant difference of the CNC samples was the appearance of the band at 1730 $cm^{-1}$ related to carbonyl groups (C=O) from hemicellulose or esterification of cellulose. CNCs exhibited lower thermal stability than the original fiber due to the disruption of crystalline structures and the introduction of sulfate groups in the cellulose. The crystallinity of CNCs increased due to the damage of the amorphous region of cellulose during acid

hydrolysis. This research showed that *Pennisetum hydridum* could be used as a raw material to prepare CNCs and provided a new way for resource use of *Pennisetum hydridum* fertilized by MSS, although more studies regarding process optimization, the recovery rate of acid, and end uses for CNC products are needed. In future research, we will use CNCs obtained from *Pennisetum hydridum* as the adsorbent of heavy metals of wastewater or washing agent of heavy metal–contaminated soil.

## DATA AVAILABILITY STATEMENT

The original contributions presented in the study are included in the article/supplementary material, and further inquiries can be directed to the corresponding author.

## AUTHOR CONTRIBUTIONS

XY have carried out the CNC preparation experiments and YJ have carried out the detailed characterization of the products. QW, ZW and XL have corrected and edited manuscript. YC supported the project financially, reviewed and edited the manuscript.

## FUNDING

## REFERENCES

Agarwal, U. (2015). Tailoring the Yield and Characteristics of wood Cellulose Nanocrystals (CNC) Using Concentrated Acid Hydrolysis. *Cellulose* 22 (3), 1753–1762. doi:10.1007/s10570-015-0615-1

Bano, S., and Negi, Y. S. (2017). Studies on Cellulose Nanocrystals Isolated from Groundnut Shells. *Carbohydr. Polym.* 157, 1041–1049. doi:10.1016/j.carbpol.2016.10.069

Beck-Candanedo, S., Roman, M., and Gray, D. G. (2005). Effect of Reaction Conditions on the Properties and Behavior of wood Cellulose Nanocrystal Suspensions. *Biomacromolecules* 6 (2), 1048–1054. doi:10.1021/bm049300p

Camarero Espinosa, S., Kuhnt, T., Foster, E. J., and Weder, C. (2013). Isolation of Thermally Stable Cellulose Nanocrystals by Phosphoric Acid Hydrolysis. *Biomacromolecules* 14 (4), 1223–1230. doi:10.1021/bm400219u

Chen, X., Deng, X., Shen, W., and Liang, J. (2012). Controlled Enzymolysis Preparation of Nanocrystalline Cellulose from Pretreated Cotton Fibers. *Bioresources* 7 (3), 4237–4248.

Chen, Y., Jiang, Y., Wan, J., Wu, Q., Wei, Z., and Ma, Y. (2018). Effects of Wet-Pressing Induced Fiber Hornification on Hydrogen Bonds of Cellulose and on Properties of eucalyptus Paper Sheets. *Holzforschung* 72 (10), 829–837. doi:10.1515/hf-2017-0214

Chen, Y., Wan, J., Dong, X., and Ma, Y. (2013). Fiber Properties of eucalyptus Kraft Pulp with Different Carboxyl Group Contents. *Cellulose* 20, 2839–2846. doi:10.1007/s10570-013-0055-8

Culsum, N. T. U., Melinda, C., Leman, I., Wibowo, A., and Budhi, Y. W. (2021). Isolation and Characterization of Cellulose Nanocrystals (CNCs) from Industrial Denim Waste Using Ammonium Persulfate. *Mater. Today Commun.* 26, 101817. doi:10.1016/j.mtcomm.2020.101817

Dai, S. (2011). *Fabrication, Characterization and Application of Nancellulose from Hemp Fibres.* Fuzhou, China: Dissertation, Fujian Agriculture and Forestry University.

Deepa, B., Abraham, E., Cordeiro, N., Mozetic, M., Mathew, A. P., Oksman, K., et al. (2015). Utilization of Various Lignocellulosic Biomass for the Production of Nanocellulose: a Comparative Study. *Cellulose* 22, 1075–1090. doi:10.1007/s10570-015-0554-x

Gao, B. B. (2011). Summarization of Nano-Cellulose. *Value Eng.* 30 (34), 272–273.

Gu, J., Catchmark, J. M., Kaiser, E. Q., and Archibald, D. D. (2013). Quantification of Cellulose Nanowhiskers Sulfate Esterification Levels. *Carbohydr. Polym.* 92 (2), 1809–1816. doi:10.1016/j.carbpol.2012.10.078

Habibi, Y., Lucia, L. A., and Rojas, O. J. (2010). Cellulose Nanocrystals: Chemistry, Self-Assembly, and Applications. *Chem. Rev.* 110, 3479–3500. doi:10.1021/cr900339w

He, H., Pan, J., Yu, P., Chen, G., and Li, H. (2017). Effects of Hybrid Giant Napier Biochar on Cadmium Migration in a Cabbage-Soil System Contaminated with

Cadmium and Butachlor. *Pol. J. Environ. Stud.* 26 (2), 619–625. doi:10.15244/pjoes/65362

He, L., Zhu, Q. L., Wang, Y. W., He, M. X., and Tan, F. R. (2020). Advances in Research on the Comprehensive Utilization of a Perennial Grass Pennisetum Hydridum. *Chin. J. Appl. Environ. Biol.* 26 (3), 705–712.

Huang, Z. J., Zhu, Z. A., Wu, X. S., Lai, X. L., Wang, P. Y., Hu, X. J., et al. (2016). Adsorption of Heavy Metals by Biochar Derived from *Pennisetum* Sinese Roxb. *Environ. Chem.* 35 (4), 766–772.

Jiang, Y., Wu, Q., Wei, Z., Wang, J., Fan, Z., Pang, Z., et al. (2019). Papermaking Potential of Pennisetum Hybridum Fiber after Fertilizing Treatment with Municipal Sewage Sludge. *J. Clean. Prod.* 208, 889–896. doi:10.1016/j.jclepro.2018.10.148

Kargarzadeh, H., Ahmad, I., Abdullah, I., Dufresne, A., Zainudin, S. Y., and Sheltami, R. M. (2012). Effects of Hydrolysis Conditions on the Morphology, Crystallinity, and thermal Stability of Cellulose Nanocrystals Extracted from Kenaf Bast Fibers. *Cellulose* 19 (3), 855–866. doi:10.1007/s10570-012-9684-6

Kontturi, E., Meriluoto, A., Penttilä, P. A., Baccile, N., Malho, J.-M., Potthast, A., et al. (2016). Degradation and Crystallization of Cellulose in Hydrogen Chloride Vapor for High-Yield Isolation of Cellulose Nanocrystals. *Angew. Chem. Int. Ed.* 55, 14455–14458. doi:10.1002/anie.201606626

Lin, X. Y., Wang, H., Wang, H., Chen, C., Wu, Q. T., Wei, Z. B., et al. (2015). Using Hybrid Giant Napier to Treat Municipal Sewage Sludge and Produce Plant Biomass. *Acta Ecol. Sin* 35 (12), 4324–4240. doi:10.5846/stxb201311042658

Liu, C., Du, H. S., Yu, G., Zhang, Y. D., Kong, Q. S., Li, B., et al. (2017). Simultaneous Extraction of Carboxylated Cellulose Nanocrystals and Nanofibrils via Citric Acid Hydrolysis—A Sustainable Route. *Pap. Biomater.* 2 (4), 19–26.

Liu, H., Du, H., Zheng, T., Liu, K., Ji, X., Xu, T., et al. (2021). Cellulose Based Composite Foams and Aerogels for Advanced Energy Storage Devices. *Chem. Eng. J.* 426, 130817. doi:10.1016/j.cej.2021.130817

Liu, K., Du, H., Zheng, T., Liu, H., Zhang, M., Zhang, R., et al. (2021). Recent Advances in Cellulose and its Derivatives for Oilfield Applications. *Carbohydr. Polym.* 259, 117740. doi:10.1016/j.carbpol.2021.117740

Liu, W., Du, H., Zhang, M., Liu, K., Liu, H., Xie, H., et al. (2020). Bacterial Cellulose-Based Composite Scaffolds for Biomedical Applications: a Review. *ACS Sustainable Chem. Eng.* 8, 7536–7562. doi:10.1021/acssuschemeng.0c00125

Ma, C. J., Ming, H., and Li, H. S. (2013). Study of Red Mud Improvement with the Mixing Method and the Impact of Pennisetum Hybridum Plantation on Red Mud Amendment. *Amr* 807-809, 392–401. doi:10.4028/www.scientific.net/amr.807-809.392

Ma, C., Naidu, R., Liu, F., Lin, C., and Ming, H. (2012). Influence of Hybrid Giant Napier Grass on Salt and Nutrient Distributions with Depth in a saline Soil. *Biodegradation* 23 (6), 907–916. doi:10.1007/s10532-012-9583-4

Mao, H. Q., Gong, Y. Y., Liu, Y. L., Wang, S. Q., and Du, L. L. (2017). Progress in Nanocellulose Preparation and Application. *Pap. Biomater.* 2 (4), 65–76.

Morais, J. P. S., Rosa, M. d. F., de Souza Filho, M. d. S. M., Nascimento, L. D., do Nascimento, D. M., and Cassales, A. R. (2013). Extraction and Characterization of Nanocellulose Structures from Raw Cotton Linter. *Carbohydr. Polym.* 91, 229–235. doi:10.1016/j.carbpol.2012.08.010

Mukherjee, S. M., and Woods, H. J. (1953). X-ray and Electron Microscope Studies of the Degradation of Cellulose by Sulphuric Acid. *Biochim. Biophys. Acta* 10, 499–511. doi:10.1016/0006-3002(53)90295-9

Nickerson, R. F., and Habrle, J. A. (1947). Cellulose Intercrystalline Structure. *Ind. Eng. Chem.* 39 (11), 1507–1512. doi:10.1021/ie50455a024

Nurain, J., Ishak, A., and Alain, D. (2012). Extraction, Preparation and Characterization of Cellulose Fibres and Nanocrystals from rice Husk. *Ind. Crop Prod.* 37 (1), 93–99. doi:10.1016/j.indcrop.2011.12.016

Peng, N. M., Chen, X. R., Zhang, R. X., and Zheng, M. J. (2010). The Cultivation and Comprehensive Utilization Technology of Hybrid Giant Napier. *Mod. Agric. Sci. Technol.* (8), 348–358.

Phanthong, P., Reubroycharoen, P., Hao, X., Xu, G., Abudula, A., and Guan, G. (2018). Nanocellulose: Extraction and Application. *Carbon Resour. Convers.* 1 (1), 32–43. doi:10.1016/j.crcon.2018.05.004

Qin, F. Y. (2018). *Study on Zeta Potential Measurement Based on Phase Analysis Light Scattering.* Zibo, China: Dissertation, Shandong University of Technology.

Ru, J., Geng, B. Y., Tong, C. C., Wang, H. Y., Wu, S. C., and Liu, H. Z. (2017). Nanocellulose-based Adsorption Materials. *Prog. Chem.* 29 (10), 1228–1251. doi:10.7536/PC170616

Tang, L. R., Ou, W., Lin, W. Y., Chen, Y. D., Chen, X. R., and Huang, B. (2011). Optimization of Acid Hydrolysis Processing of Nanocellulose crystal Using Response Surface Methodology. *Chem. Ind. Prod.* 31 (6), 61–65.

Tang, Y., Yang, S., Zhang, N., and Zhang, J. (2014). Preparation and Characterization of Nanocrystalline Cellulose via Low-Intensity Ultrasonic-Assisted Sulfuric Acid Hydrolysis. *Cellulose* 21 (1), 335–346. doi:10.1007/s10570-013-0158-2

Vanderfleet, O. M., Osorio, D. A., and Cranston, E. D. (2018). Optimization of Cellulose Nanocrystal Length and Surface Charge Density through Phosphoric Acid Hydrolysis. *Phil. Trans. R. Soc. A* 376 (2112), 20170041. doi:10.1098/rsta.2017.0041

Visanko, M., Liimatainen, H., Sirviö, J. A., Heiskanen, J. P., Niinimäki, J., and Hormi, O. (2014). Amphiphilic Cellulose Nanocrystals from Acid-free Oxidative Treatment: Physicochemical Characteristics and Use as an Oil-Water Stabilizer. *Biomacromolecules* 15 (7), 2769–2775. doi:10.1021/bm500628g

Wang, H. K. (2013). Preparation, Characterization and Application of Nano Cellulose Fibrils from Bamboo. *Dissertation, Chinese Academy of Forestry, Beijing, China.*

Wang, Q., Zhao, X., and Zhu, J. Y. (2014). Kinetics of Strong Acid Hydrolysis of a Bleached Kraft Pulp for Producing Cellulose Nanocrystals (CNCs). *Ind. Eng. Chem. Res.* 53 (27), 11007–11014. doi:10.1021/ie501672m

Wang, X. N., Yi, Z. C., Zhang, Y. F., Wang, J. Q., Zhang, Y. J., and Li, H. S. (2015). Responses and Remediating Effects of *Pennisetum Hydridum* to Application of Heavy-Metals-Contaminated Chicken Manures and Sewage Sludges. *J. Agric. Resour. Environ.* 32 (5), 477–484. doi:10.13254/j.jare.2015.0064

Widsten, P., Dooley, N., Parr, R., Capricho, J., and Suckling, I. (2014). Citric Acid Crosslinking of Paper Products for Improved High-Humidity Performance. *Carbohydr. Polym.* 101, 998–1004. doi:10.1016/j.carbpol.2013.10.002

Xie, H., Zhao, X. M., Xie, Z., Wu, K. Q., Li, X. L., Yang, R. G., et al. (2016). Phytoremediation Efficiency of *Pennisetum Hydridum* for Acid- and Cadmium-Polluted Soil and its Safe Utilization. *J. Agric. Resour. Environ.* 35 (3), 478–484. doi:10.11654/jaes.2016.03.010

Xu, W. Y., Fu, S. Y., Peng, Y. Y., and Liu, H. (2016). Preparation of Nanocellulose from Three Typical Plants in the South Area. *J. Dalian Polytech Uni* 35 (5), 347–352.

Xu, W. Y. (2016). *The Research of Nanocellulose Fiber Raw Material Preparation.* Dissertation, South China University of Technology, Guangzhou, China.

Yi, Z. C., He, J. B., Cheng, H., Lu, S. M., He, H. Z., Zhang, W. Q., et al. (2014). Effects of Cd Polluted Soil on the Modular Growth and Physiological Characteristics of *Pennisetum Hydridum.* *J. Agric. Resour. Environ.* 33 (2), 276–282.

Zhao, T., Jiang, C. A., Qiu, J. R., Wang, X. J., Zeng, J. W., and Zhou, Z. H. (2017). Research on Adsorption Properties of Sulfonamides in Aqueous Solution by *Pennisetum Hydridum* Derived Biochar. *Technol. Water Treat.* 43 (4), 56–65. doi:10.16796/j.cnki.1000-3770.2017.04.013

Zhao, Y. H., Lun, Y. H., Chen, W., and Jiang, Q. (2015). Research on the Comprehensive Exploitation and Utilization of Hybrid Giant Napier. *J. Yichun Coll.* 37 (9), 89–91.